Observational Study

Medicine®

OPEN

Value of virtual monochromatic spectral images with metal artifact reduction algorithm in dual-energy computed tomography-guided microcoil localization of pulmonary nodules

Zhuo Liu, BS, Zhuolu Zhang, MD, Chen Chen, MD, Nan Hong, MD*

Abstract

To evaluate the clinical value of virtual monochromatic spectral (VMS) images with metal artifact reduction (MAR) algorithm in dual-energy computed tomography (DECT)-guided microcoil localization of pulmonary nodules.

Fifty-one patients underwent DECT after placement of microcoils on small pulmonary nodules before video-assisted thoracoscopic surgery (VATS). Optimal energy level (in keV) was defined as the level at which CT values of nodules were equivalent to those of 120 kVp images and with no serious metal artifacts. VMS images at optimal keV and at 50, 90,110, and 140 keV with and without MAR were reconstructed. Image quality was scored using a 3-point scale: 1 = excellent, minimal artifacts; 2 = good, mild artifacts; and 3 = poor, extensive artifacts. Image quality scores between the VMS-only and VMS + MAR groups were compared;

74 keV was found to be the optimal level for VMS images. The image quality of the VMS + MAR images at 74 keV were significantly better than VMS-only images (1.35 ± 0.59 vs 2.11 ± 0.87, $P = .005$). There was no difference in image quality score among VMS + MAR images at 74 keV and higher energy levels.

VMS images from DECT at 74 keV with MAR can reduce artifacts from microcoils and improve image quality for microcoil localization of pulmonary nodules.

Abbreviations: DECT = dual-energy computed tomography, MAR = metal artifact reduction, SECT = single-energy computed tomography, VATS = video-assisted thoracoscopic surgery, VMS = virtual monochromatic spectral.

Keywords: dual-energy CT, lung nodule, metal artifact, microcoil, preoperative localization

1. Introduction

In recent years, the video-assisted thoracoscopic surgery (VATS) has gradually substituted the traditional thoracotomy as routine therapy for lung nodules lesion.[1] However, since up to 54% of small lung nodules cannot be localized accurately via observation or palpation in VATS, and require the conversion to thoracotomy. Moreover, nodules with diameter of less than 10 mm and with distance more than 5 mm from pleura are sometimes difficult to localize accurately even through the thoracotomy.[2] Therefore, the localization of lung nodules is especially important to making the pre-surgical planning and smoothly completing the surgery, and the computed tomography(CT)-guided microcoil localization is one of the preferred methods.[3]

Since the microcoil is often made of such metals as platinum, metal artifacts are generally produced in the conventional CT images that seriously influence the display of microcoil. Metal artifacts seriously impair the precise localization of the microcoil and prevent the surgeons from understanding the accurate position relation between microcoil and nodules.[4] The combination of dual-energy CT scanning and metal artifact reduction (MAR) algorithm provides a way to effectively reduce artifacts caused by metals in CT images. Our study aimed to explore the value of virtual monochromatic spectral (VMS) images with MAR on reducing microcoil-induced metal artifacts for the accurate microcoil localization of lung nodules.

2. Materials and methods

This prospective study was approved by our institutional review board. We obtained informed consent from all patients.

2.1. Subjects and localization operation

Fifty-one patients who underwent CT-guided lung nodules microcoil localization were analyzed retrospectively. Nodules were deemed to be eligible for the study when they were located within 4 cm of a pleural surface or fissure; showed no evidence of hilar, mediastinal, chest wall, or diaphragmatic invasion. A platinum tower-shaped microcoil (Cook, Bloomington, IN) was used as localization metal marker. The microcoil was placed percutaneously through a 22-gauge needle into the lung tissue near the nodule and the microcoil tail coiled on the visceral pleural surface near the foci to form a tailing phenomenon. During the localization, a single-energy CT (SECT) scanning was

Editor: Weisheng Zhang.

The authors declare no conflicts of interest.

Department of Radiology, People's Hospital, Peking University, Beijing, China.

* Correspondence: Nan Hong, Department of Radiology, People's Hospital, Peking University, Beijing, China (e-mail: hongnanrmyy@sina.cn).

Medicine (2018) 97:29(e11562)

Received: 30 November 2017 / Accepted: 22 June 2018

http://dx.doi.org/10.1097/MD.0000000000011562

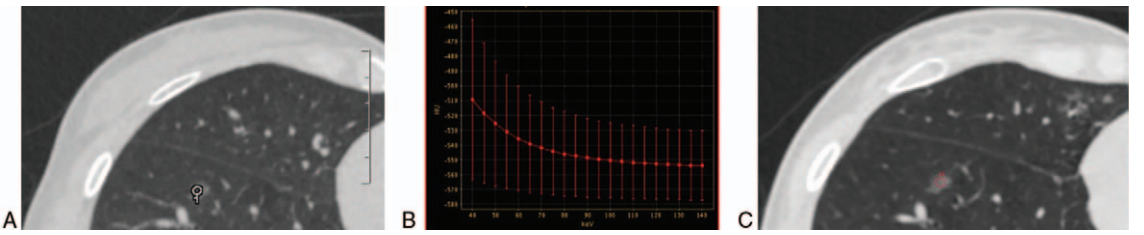

Figure 1. Images of 74 keV virtual monochromatic spectral (VMS): the CT value of lung nodules was closest to that of the 120 kVp image. Image (A) (120 kVp): the CT value of a lung nodule was –544.6 HU. Image (B) (spectral curve of lung nodules): the CT value of the same lung nodule as function of photon energy, decreasing with the increase of keV value. Image (C) (74 keV): the CT value of the lung nodule was –544.5 HU.

applied. After the placement of microcoil, the DECT scanning was applied to evaluate the localization effect.

2.2. Scanning equipment and parameters

All patients were scanned using a dual-energy CT scanner (Revolution CT; GE Healthcare, Waukesha, WI). Parameters for SECT scanning during the localization were: 120 kVp tube voltage; tube current automatically modulated during scans to achieve a preset noise index (NI) of 30 HU; 0.28 seconds gantry rotation time; 80 mm collimation width; and 1.531:1 pitch. Parameters for DECT scanning after the placement of microcoil were: fast switching between 80 kVp and 140 kVp tube voltages; 200 mA tube current; 0.5 seconds gantry rotation time; 80 mm collimation width; and 1.531:1 pitch; 1.25 mm thickness.

2.3. Image reconstruction and optimal energy level selection in DECT

DECT images were first reconstructed using the standard kernel to generate 101 sets of virtual monochromatic spectral (VMS) images with photon energies from 40 to 140 keV. These images were transferred to an Advanced Workstation (AW 4.7; GE Healthcare) together with the conventional 120 kVp images for selecting the optimal energy level for further processing. An optimal energy level was defined as the energy level at which CT values of nodules measured on the VMS images were equivalent to those in the conventional 120 kVp images. A region-of-interest (ROI) was placed on nodule as large as possible to measure CT value and to generate a spectral HU curve (CT value as a function of photon energy) in DECT images as shown in Figure 1 using the Gemstone Spectral Imaging (GSI) Viewer software. The keV value on the curve where the CT value of lung nodules was closest to that on the 120 kVp images was selected as the optimal energy level and recorded. If the keV values of all nodules follow normal distribution, the average would be selected as the optimal keV level for the patient population. DECT images were then reconstructed with (VMS + MAR) and without (VMS-only) MAR algorithm at the optimal keV, as well as at energy levels of 50 keV, 90 keV, 110 keV, and 140 keV.

2.4. Evaluation method

The image quality in terms of the severity of metal artifacts, accurate localization of microcoil and nodule and the clarity of the relationship between microcoil and nodule were scored by 2 diagnostic radiologists double blindly using a 3-point scoring system. The quality of images was evaluated as follows: excellent, lack of metal artifact, clear display of microcoil and its relationship with lung nodules and pleura; good, some metal artifacts not influencing the display of microcoil and its relationship with lung nodules and pleura; and poor, severe metal artifacts seriously influencing the display of microcoil and its relationship with lung nodules and pleura. The evaluation criterion and sample image comparison were shown in Figures 2–6.

2.5. Statistical analysis

Data were statistically analyzed using SPSS 20.0 software; Chicago, Ill. The subjective image quality scores between the VMS-only and VMS + MAR groups were evaluated using the paired Mann–Whitney U test. $P < .05$ indicated a difference of statistical significance. The consistency of results between the 2 readers was evaluated using the Kappa analysis: poor ($K < 0.40$); moderate ($0.40 \leq K < 0.75$); and good ($K \geq 0.75$).

3. Results

A total of 51 lung nodules underwent the localization procedure successfully in the first try. After the localization, the microcoil did not displace or fall off, and VATS were completed successfully and smoothly.

The optimal photon energy level was 74.0 ± 5.7 keV (60–83 keV), and was found to follow normal distribution. The 74 keV was then selected as the optimal energy level for the study. The subjective image quality scores of the DECT images reconstructed with MAR algorithm (VMS + MAR images) at 50 keV, 74 keV, 90 keV, 110 keV, and 140 keV were 1.51 ± 0.67, 1.35 ± 0.59, 1.33 ± 0.50, 1.32 ± 0.49, and 1.32 ± 0.56, respectively. As compared with other images, the VMS + MAR images at 50 keV had more serious metal artifacts, significantly higher image noise and statistically worse score ($P < .05$). Between the VMS + MAR images at 74 keV and energy levels higher than 74 keV (ie, 90 keV, 110 keV, and 140 keV), the image quality scores and metal artifact severity were not significantly different (all $P > .05$). (Fig. 7)

For images at the optimal energy level of 74 keV, the subjective score was 2.11 ± 0.87 and 1.35 ± 0.59 for the VMS-only and VMS + MAR images, respectively ($P = .005$), with good consistency between the 2 readers ($k = 0.78$) (Figs. 2–6). Three were 8 patients where the lung nodules in the VMS-only images were seriously influenced by metal artifacts so that the position of nodules could not be determined because the microcoil head was at a too small distance from lung nodules. The metal artifacts were significantly reduced in the VMS+MAR images and the lung nodules were clearly displayed.

4. Discussion

In recent years, VATS has gradually substituted the traditional thoracotomy as a preferred choice for excising small lung

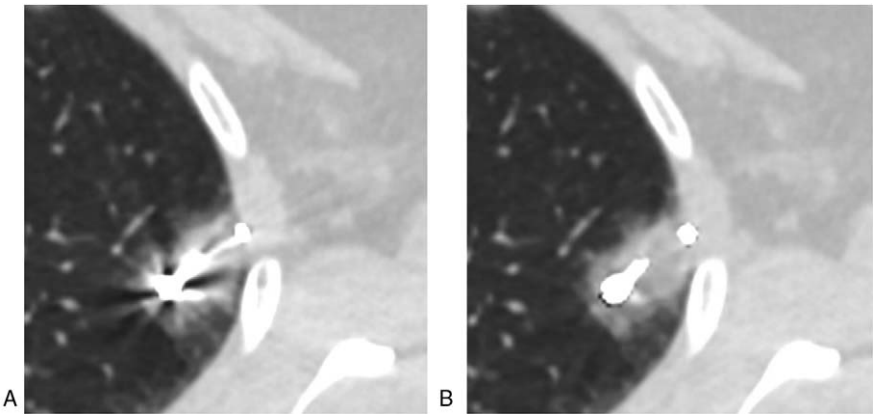

Figure 2. Localization with microcoil tailing: the microcoil head was released at the lung tissues near the nodules, but the microcoil tail was coiled on visceral pleural surface. Image (A) (VMS-only image): serious metal artifacts, unclear display of microcoil head/tail, poor image quality (score of 3). Image (B) (VMS + MAR image): metal artifacts greatly reduced, clear display of microcoil head/tail, excellent image quality (score of 1).

nodules. VATS has many advantages: micro incision, small volume of excised lung lobe, less peri-surgical complications, and short hospitalization duration. However, since lung nodules often have small volume, less solid substances and soft texture, most of them cannot be localized accurately via observation or palpation in VATS, and only the traditional thoracotomy is feasible. With advances in diagnostic performance, CT examination has become a reliable and reproducible imaging modality for cancer screening, treatment planning and follow up examination,[5–7] meanwhile CT also plays an important role for localization of small peripheral pulmonary nodules prior to VATS resection using the implantation of microcoils. As verified by numerous literatures, the CT-guided placement of metal marker (eg, platinum microcoil) is one of the safe and effective localization means.[8–10] By retaining the microcoil in the lung tissues near foci during the localization, not only the localization accuracy is not influenced, but also the tumor is not spread along the needle track during the puncturing operation, and the pathologic examination will not be influenced by the microcoil. In VATS, the lung nodules can be localized accurately for guiding the foci excision through the finger palpation, perspective imaging and direct observation of microcoil tail retained at visceral pleural surface. After the excision of foci, the small lung nodules can be easily found from the isolated specimen according to the position of microcoil, so as to facilitate the collection of pathological material. Therefore, it is the key for success in subsequent surgery and biopsy by confirming the localization effect and clearly displaying the position relationship between the microcoil and lung nodules or pleura. Unfortunately, the microcoil generally forms a metal artifact in CT images, which seriously influences the diagnoses.[11,12]

DECT scanning refers to simultaneous acquisition of low and high peak voltage CT data. There is an increased interest in DE scanning, driven by the recent commercial availability of different DE hardware platforms.[13,14] The VMS images obtained through DECT scanning simulate the images obtained by single-energy photons[15,16] to have much less beam hardening artifacts.[17] Moreover, the data loss caused by a phenomenon of photon hunger produced during the passing of x-ray through metal can be corrected by MAR. Therefore, the MAR-treated

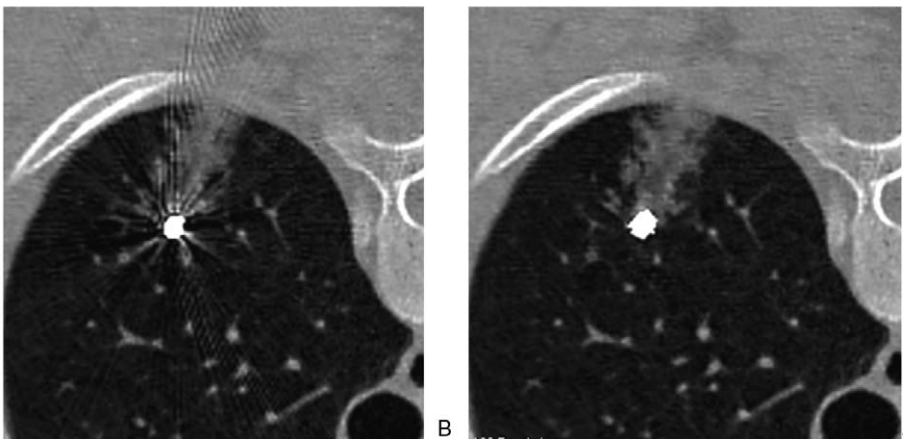

Figure 3. Hemorrhage caused by the puncturing. Image (A) (VMS-only image): some metal artifacts not seriously influencing the visualization for hemorrhage, good image quality (score of 2). Image (B) (VMS + MAR image): metal artifacts greatly reduced, clear display of microcoil head and hemorrhage, excellent image quality (score of 1).

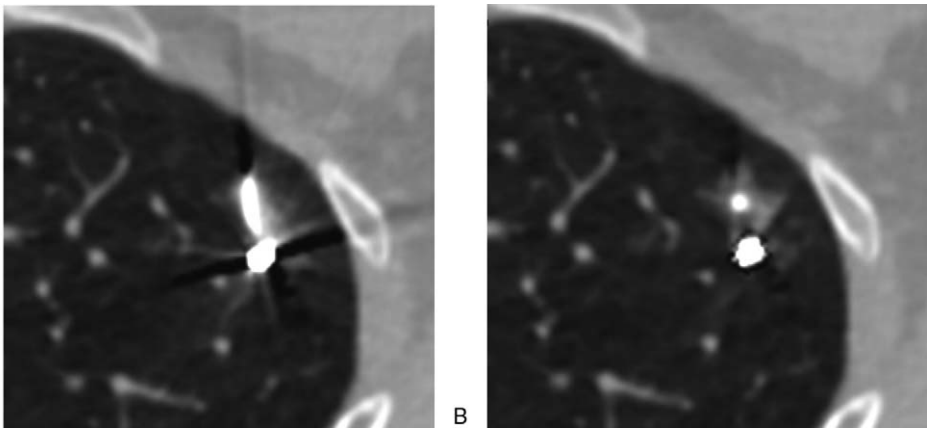

Figure 4. Hemorrhage caused by the puncturing. Image (A) (VMS-only image): severe metal 4artifacts seriously influencing the visualization for hemorrhage, poor image quality (score of 3). Image (B) (VMS + MAR image): metal artifacts greatly reduced, clear display of hemorrhage, excellent image quality (score of 1).

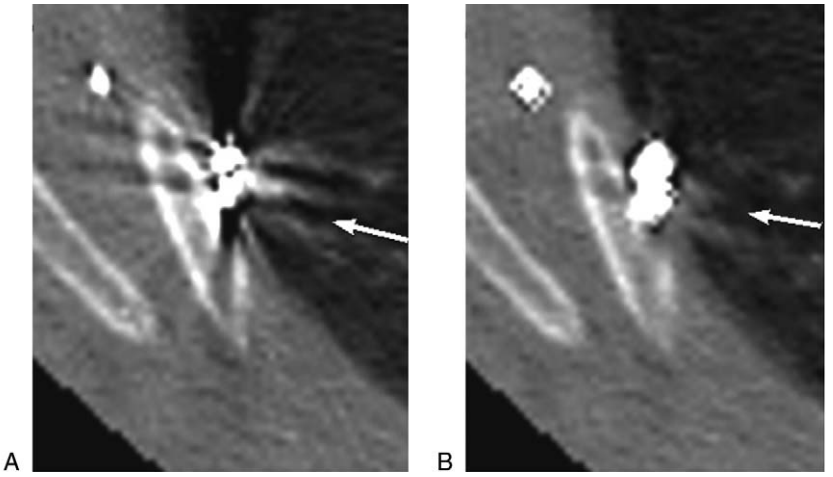

Figure 5. Nodule adjacent to the pleura, microcoil localization on visceral pleural surface near the nodule. Image (A) (VMS-only image): concealment of nodules (as directed by arrow) and pleura by metal artifact, non-judgment on whether the microcoil head was placed on visceral pleural surface near the nodules, poor image quality (score of 3). Image (B) (VMS + MAR images): metal artifacts greatly reduced, more clear display of nodules (as directed by arrow), pleura and rib, excellent image quality (score of 1).

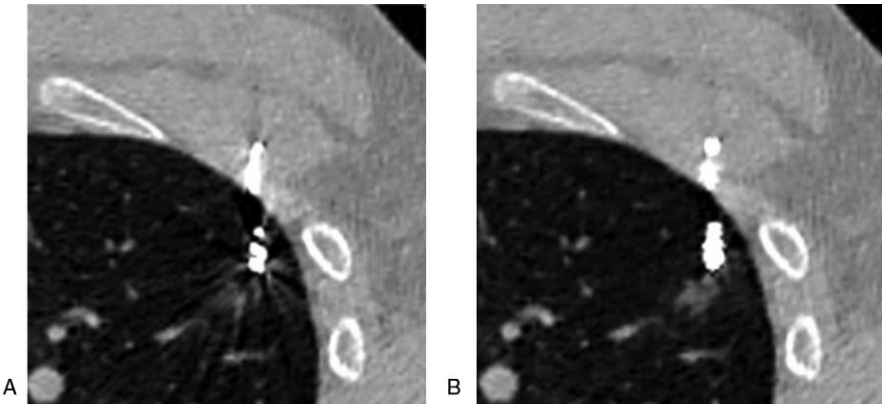

Figure 6. Nodules adjacent to microcoil head. Image (A) (VMS-only image): concealment of nodules by metal artifact, poor image quality (score of 3). Image (B) (VMS + MAR image): metal artifacts greatly reduced, excellent image quality (1 score).

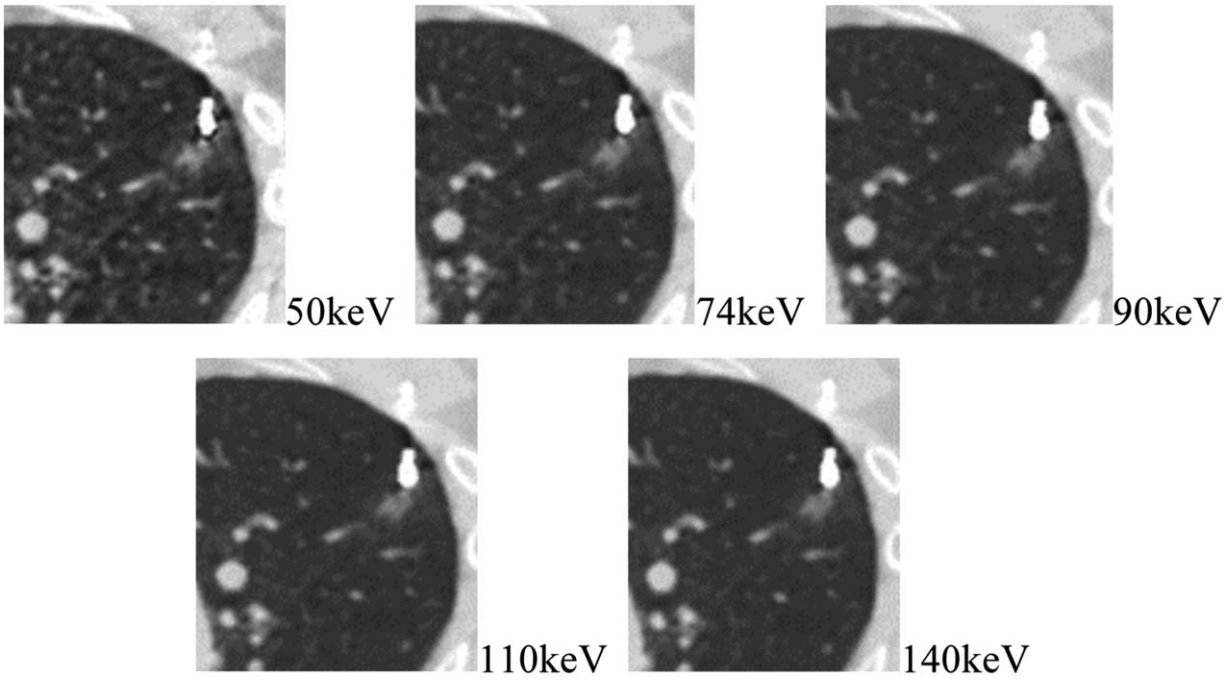

Figure 7. VMS + MAR images at 50 keV, 74 keV, 90 keV, 110 keV, and 140 keV: as compared with other images, the VMS + MAR images at 50 keV had a more serious metal artifact and a higher image noise; between the VMS + MAR images at 74 keV and higher energy levels, the severities of metal artifact were not significantly different.

VMS images (VMS + MAR images) can theoretically effectively inhibit the metal artifacts caused by the platinum microcoil,[18–21] and was demonstrated in our study. As shown in our study, the metal artifacts of the microcoil in the VMS + MAR images were effectively inhibited, and the display of such structures as the nearby lung tissue, pleura and nodules was significantly improved. The lung nodules in the VMS-only images in 8 patients were concealed by metal artifacts and thus displayed unclearly because the microcoil head was very close to the lung nodules. In VMS + MAR images, the metal artifacts were greatly reduced and the lung nodules could be clearly displayed. In the VMS-only images, the pleural display was seriously influenced by the metal artifacts caused by the microcoil tail during the tailing localization; in the VMS + MAR images, the chest wall was well displayed to make it much easy to judge whether the microcoil tail was on the visceral pleural surface near the foci.

With the increasing of photon energy level, the metal artifact in VMS images will be alleviated gradually[22]; however, the CT value of lung nodule will also decrease gradually and this may influence the finding of nodules. Therefore, a proper energy level should be selected to inhibit the metal artifact as far as possible under the premise of clear nodules display. The optimal energy level was determined as follows: the CT value of lung nodules on VMS images was closest to that in 120 kVp images and the diagnosis was not influenced by the metal artifact. As shown by the results of our study, compared with other photon energy levels, the CT value of lung nodules in 74 keV VMS images was closest to that in 120 kVp images, and the metal artifact degree was not further decreased significantly in the VMS + MAR images at energy levels higher than 74 keV. Therefore, the optimal energy level was selected at 74 keV.

There were limitations associated with the present study. First, the long-term effects of implantation were not evaluated. Secondly, nodules with longer distance (> 4 cm) to the pleural surface were not included. Therefore, additional trials which include deeper nodules are needed.

To sum up, the 74 keV VMS + MAR images obtained in the dual-energy CT effectively inhibit the metal microcoil-induced metal artifacts to provide safe and accurate microcoil localization of pulmonary nodules.

Author contributions

Resources: Chen Chen.
Supervision: Nan Hong.
Writing – original draft: Zhuo Liu.
Writing – review & editing: Zhuolu Zhang.

References

[1] Su TH, Fan YF, Jin L, et al. CT-guided localization of small pulmonary nodules using adjacent microcoil implantation prior to video-assisted thoracoscopic surgical resection. Eur Radiol 2015;25:2627–33.
[2] Powell TI, Jangra D, Clifton JC, et al. Peripheral lung nodules: fluoroscopically guided video-assisted thoracoscopic resection after computed tomography-guided localization using platinum microcoils. Ann Surg 2004;240:481–8.
[3] Sangha BS, Rootman J, Heran MK. CT-guided microcoil localization before surgical management of an intraorbital abscess. J Vasc Interv Radiol 2012;23:1248–9.
[4] Kha LC, Hanneman K, Donahoe L, et al. Safety and efficacy of modified preoperative lung nodule microcoil localization without pleural marking: a pilot study. J Thorac Imaging 2016;31:15–22.
[5] Razek AA, Ezzat A, Azmy E, et al. Role of whole-body 64-slice multidetector computed tomography in treatment planning for multiple myeloma. Radiol Med 2013;118:799–805.
[6] Razek AAKA, Shamaa S, Lattif MA, et al. Inter-observer agreement of whole-body computed tomography in staging and response assessment in lymphoma: the Lugano classification. Pol J Radiol 2017;82:441–7.
[7] Ghobrial FEI, Eldin MS, Razek AAKA, et al. Computed tomography assessment of hepatic metastases of breast cancer with revised response evaluation criteria in solid tumors (RECIST) criteria (Version 1.1): inter-observer agreement. Pol J Radiol 2017;82:593–7.

[8] Finley RJ, Mayo JR, Grant K, et al. Preoperative computed tomography-guided microcoil localization of small peripheral pulmonary nodules: a prospective randomized controlled trial. J Thorac Cardiovasc Surg 2015;149:26–31.
[9] Donahoe LL, Nguyen ET, Chung TB, et al. CT-guided microcoil VATS resection of lung nodules: a single-centre experience and review of the literature. J Thorac Dis 2016;8:1986–94.
[10] Zuo T, Shi S, Wang L, et al. Supplement CT-guided microcoil placement for localising ground-glass opacity (GGO) lesions at "blind areas" of the conventional hook-wire technique. Heart Lung Circ 2017;26:696–701.
[11] Aissa J, Boos J, Sawicki LM, et al. Iterative metal artefact reduction (MAR) in postsurgical chest CT: comparison of three iMAR-algorithms. Br J Radiol 2017;20160778.
[12] Yasuda M, Yoshikawa K, Kato K, et al. Validation of a metal artifact reduction algorithm using 1D linear interpolation for cone beam ct after endovascular coiling therapy for cerebral aneurysms. Neuroradiol J 2014;27:742–54.
[13] Tawfik AM, Razek AA, Kerl JM, et al. Comparison of dual-energy CT-derived iodine content and iodine overlay of normal, inflammatory and metastatic squamous cell carcinoma cervical lymph nodes. Eur Radiol 2014;24:574–80.
[14] Tawfik AM, Kerl JM, Razek AA, et al. Image quality and radiation dose of dual-energy CT of the head and neck compared with a standard 120-kVp acquisition. AJNR Am J Neuroradiol 2011;32:1994–9.
[15] Pessis E, Campagna R, Sverzut JM, et al. Virtual monochromatic spectral imaging with fast kilovoltage switching: reduction of metal artifacts at CT. Radiographics 2013;33:573–83.
[16] Guggenberger R, Winklhofer S, Osterhoff G, et al. Metallic artefact reduction with monoenergetic dual-energy CT systematic ex vivo evaluation of posterior spinal fusion implants from various vendors and different spine levels. Eur Radiol 2012;22:2357–64.
[17] Pessis E, Sverzut JM, Campagna R, et al. Reduction of metal artifact with dual-energy CT virtual monospectral imaging with fast kilovoltage switching and metal artifact reduction software. Semin Musculoskelet Radiol 2015;19:446–55.
[18] Wellenberg RH, Boomsma MF, van Osch JA, et al. Quantifying metal artefact reduction using virtual monochromatic dual-layer detector spectral CT imaging in unilateral and bilateral total hip prostheses. Eur J Radiol 2017;88:61–70.
[19] Han SC, Chung YE, Lee YH, et al. Metal artifact reduction software used with abdominopelvic dual-energy CT of patients with metal hip prostheses assessment of image quality and clinical feasibility. AJR Am J Roentgenol 2014;203:788–95.
[20] Higashigaito K, Angst F, Runge VM, et al. Metal artifact reduction in pelvic computed tomography with hip prostheses comparison of virtual mono-energetic extrapolations from dual-energy computed tomography and an iterative metal artifact reduction algorithm. Invest Radiol 2015;50:828–34.
[21] Takrouri HS, Alnassar MM, Amirabadi A, et al. Metal artifact reduction added value of rapid-kilovoltage-switching dual-energy CT in relation to single-energy CT in a piglet animal model. AJR Am J Roentgenol 2015;205:W352–9.
[22] De Crop A, Casselman J, Van Hoof T, et al. Analysis of metal artifact reduction tools for dental hardware in CT scans of the oral cavity: kVp, iterative reconstruction, dual-energy CT, metal artifact reduction software: does it make a difference. Neuroradiology 2015;57:841–9.